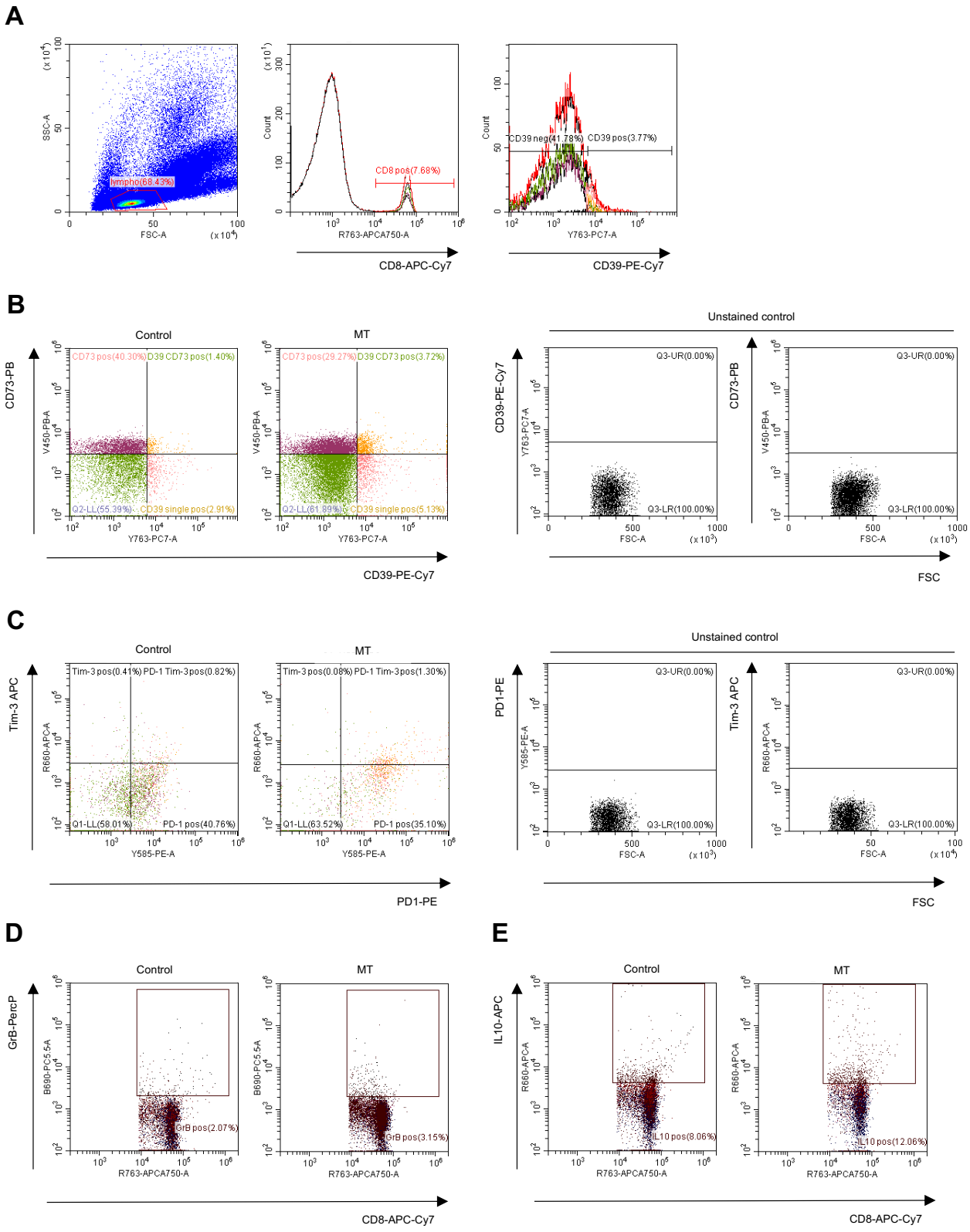
A
SSC-A
FSC-A
lmphoc(68.43%)
Count
R763-APCA750-A
CD8 pos(7.68%)
CD8-APC-Cy7
Y763-PC7-A
CD39 neg(41.78%)
CD39 pos(3.77%)
CD39-PE-Cy7
B
Control
MT
CD73-PB
V450-PB-A
CD73 pos(40.30%)
D39 CD73 pos(1.40%)
Q2-LL(55.39%)
CD39 single pos(2.91%)
CD73 pos(29.27%)
D39 CD73 pos(3.72%)
Q2-LL(61.89%)
CD39 single pos(5.13%)
CD39-PE-Cy7
Unstained control
Q3-UR(0.00%)
Q3-LR(100.00%)
FSC
C
Tim-3 APC
R660-APC-A
Tim-3 pos(0.41%) PD-1 Tim-3 pos(0.82%)
Q1-LL(58.01%)
PD-1 pos(40.76%)
Tim-3 pos(0.08%) PD-1 Tim-3 pos(1.30%)
Q1-LL(63.52%)
PD-1 pos(35.10%)
Y585-PE-A
PD1-PE
D
GrB-PercP
B690-PC5.5-A
GrB pos(2.07%)
GrB pos(3.15%)
E
IL10-APC
IL10 pos(8.06%)
IL10 pos(12.06%)

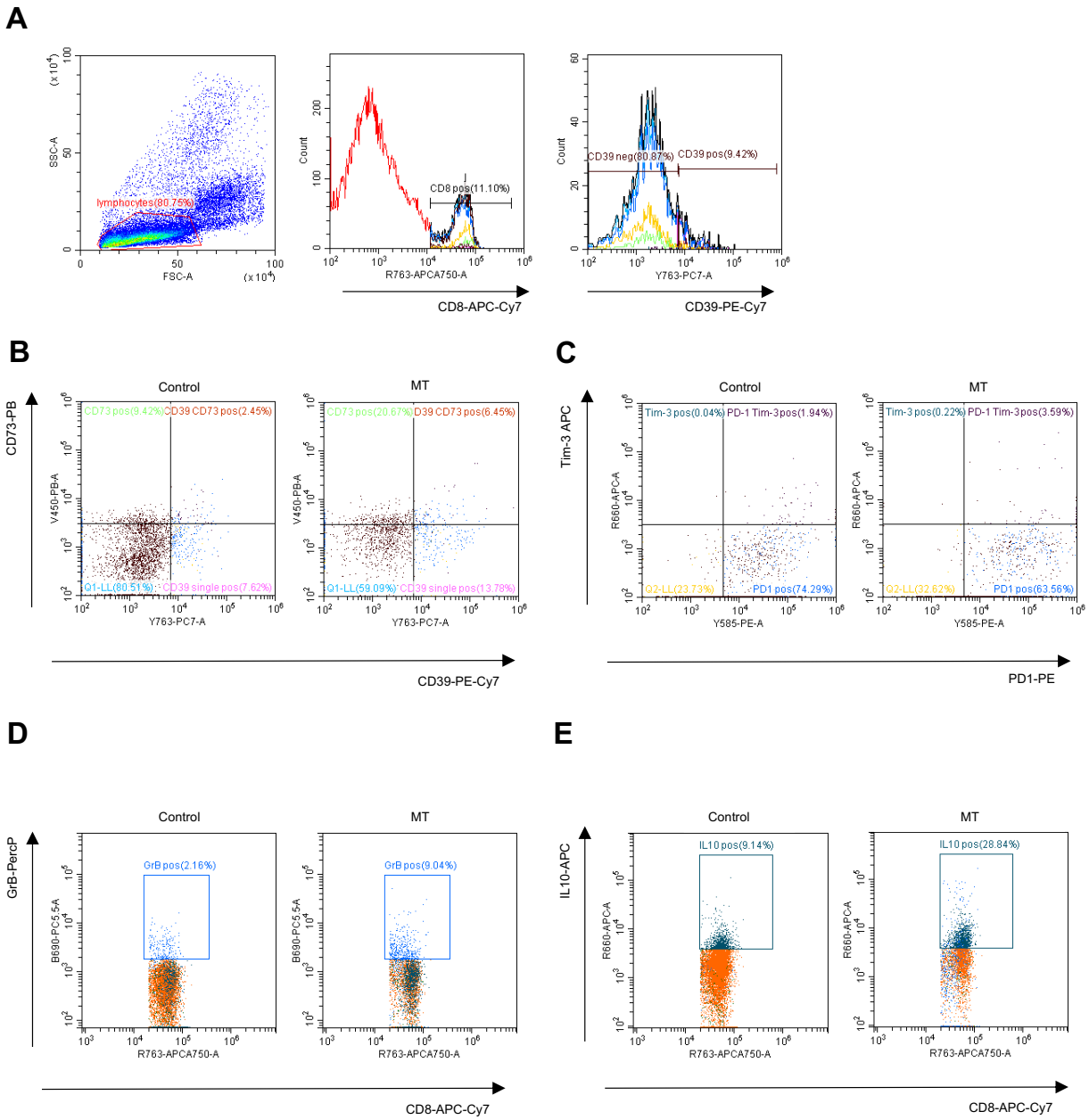
A
SSC-A
FSC-A
lymphocytes(80.75%)
Count
CD8 pos(11.10%)
R763-APCA750-A
CD8-APC-Cy7
CD39 neg(80.87%)
CD39 pos(9.42%)
Y763-PC7-A
CD39-PE-Cy7
B
Control
MT
CD73-PB
V450-PB-A
CD73 pos(9.42%)
CD39 CD73 pos(2.45%)
Q1-LL(80.51%)
CD39 single pos(7.62%)
CD73 pos(20.67%)
D39 CD73 pos(6.45%)
Q1-LL(59.09%)
CD39 single pos(13.78%)
Y763-PC7-A
CD39-PE-Cy7
C
Control
MT
Tim-3 APC
R660-APC-A
Tim-3 pos(0.04%)
PD-1 Tim-3 pos(1.94%)
Q2-LL(33.73%)
PD1 pos(74.29%)
Tim-3 pos(0.22%)
PD-1 Tim-3 pos(3.59%)
Q2-LL(33.62%)
PD1 pos(63.56%)
Y585-PE-A
PD1-PE
D
Control
MT
GrB-PercP
B690-PC5.5-A
GrB pos(2.16%)
GrB pos(9.04%)
R763-APCA750-A
CD8-APC-Cy7
E
Control
MT
IL10-APC
R660-APC-A
IL10 pos(9.14%)
IL10 pos(28.84%)
R763-APCA750-A
CD8-APC-Cy7

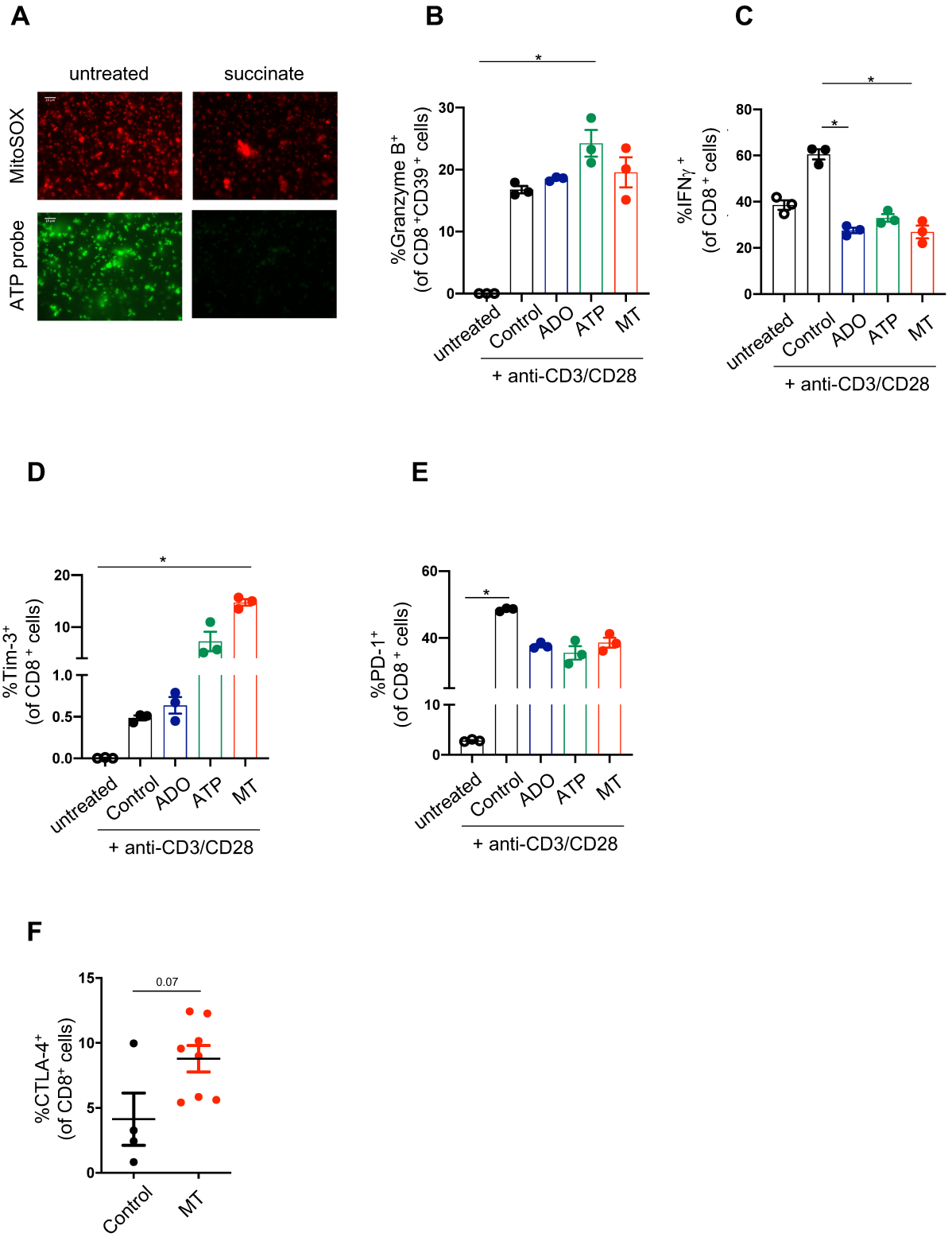
A
untreated
succinate
MitoSOX
ATP probe
B
%Granzyme B+ (of CD8+CD39+ cells)
untreated
Control
ADO
ATP
MT
+ anti-CD3/CD28
C
%IFNγ+ (of CD8+ cells)
D
%Tim-3+ (of CD8+ cells)
E
%PD-1+ (of CD8+ cells)
F
%CTLA-4+ (of CD8+ cells)
0.07

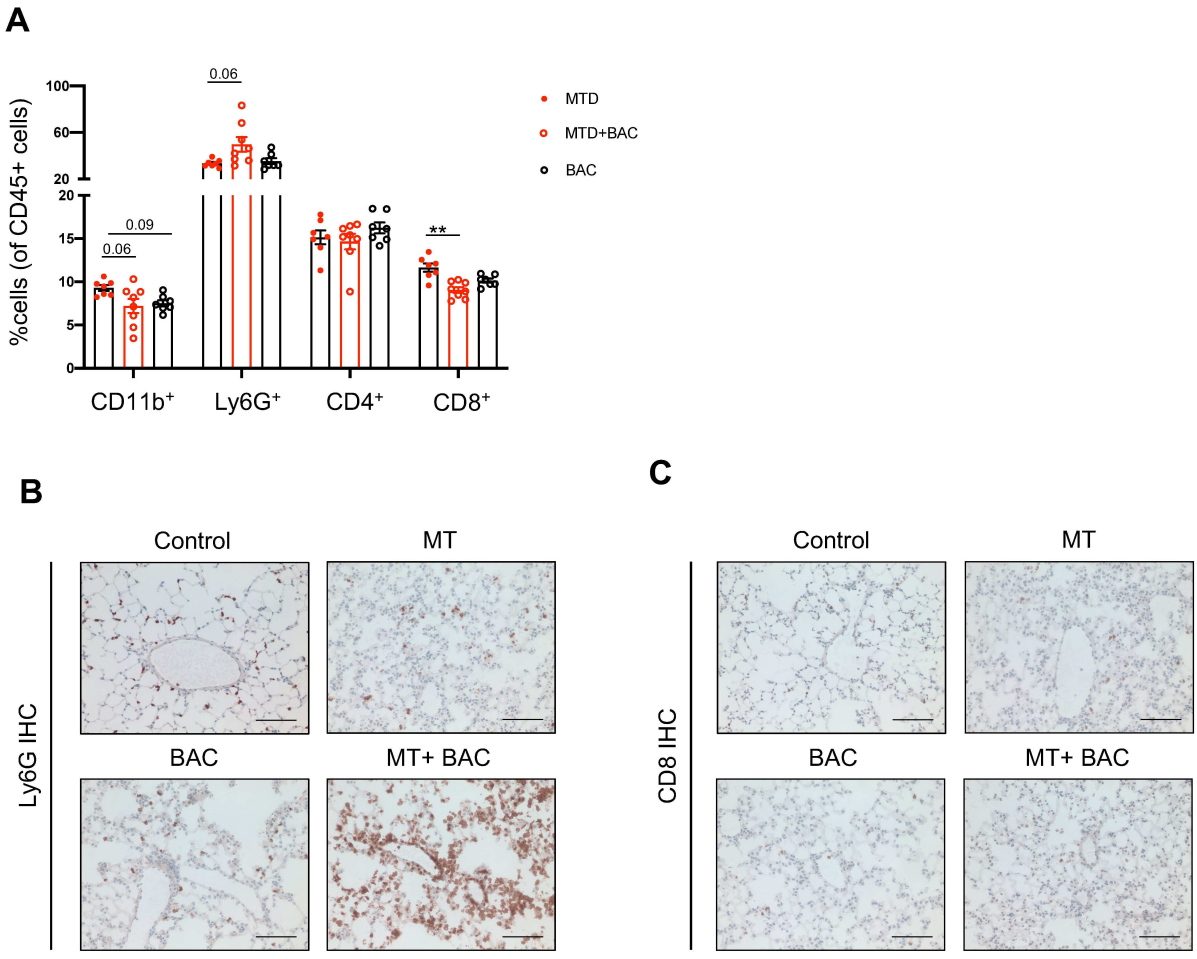
A
%cells (of CD45+ cells)
100
60
20
20
15
10
5
0
0.06
0.09
0.06
**
MTD
MTD+BAC
BAC
CD11b+
Ly6G+
CD4+
CD8+
B
Control
MT
BAC
MT+ BAC
Ly6G IHC
C
Control
MT
BAC
MT+ BAC
CD8 IHC

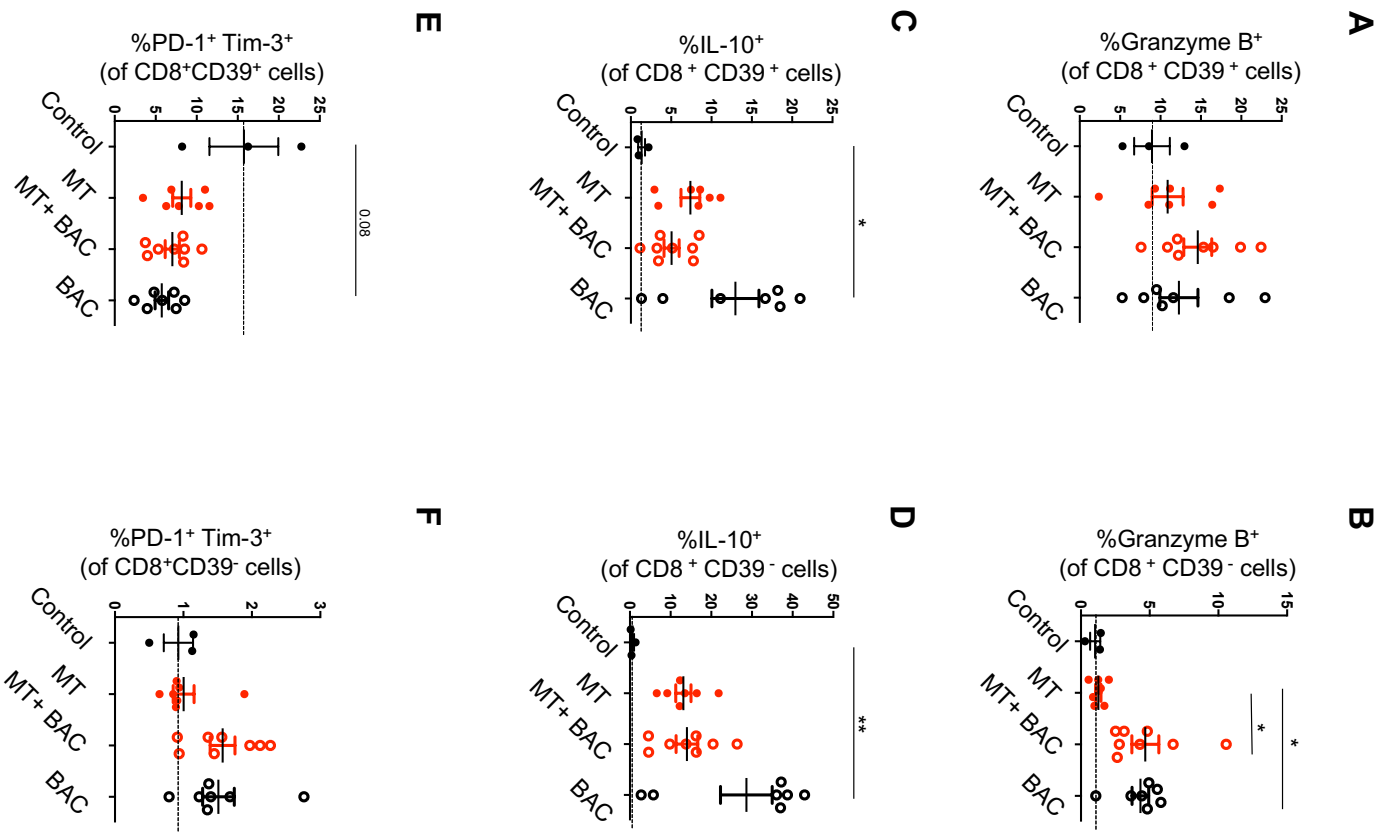
A
%Granzyme B+
(of CD8+CD39+ cells)
Control
MT
MT+ BAC
BAC
B
%Granzyme B+
(of CD8+CD39- cells)
C
%IL-10+
(of CD8+CD39+ cells)
D
%IL-10+
(of CD8+CD39- cells)
E
%PD-1+ Tim-3+
(of CD8+CD39+ cells)
0.08
F
%PD-1+ Tim-3+
(of CD8+CD39- cells)

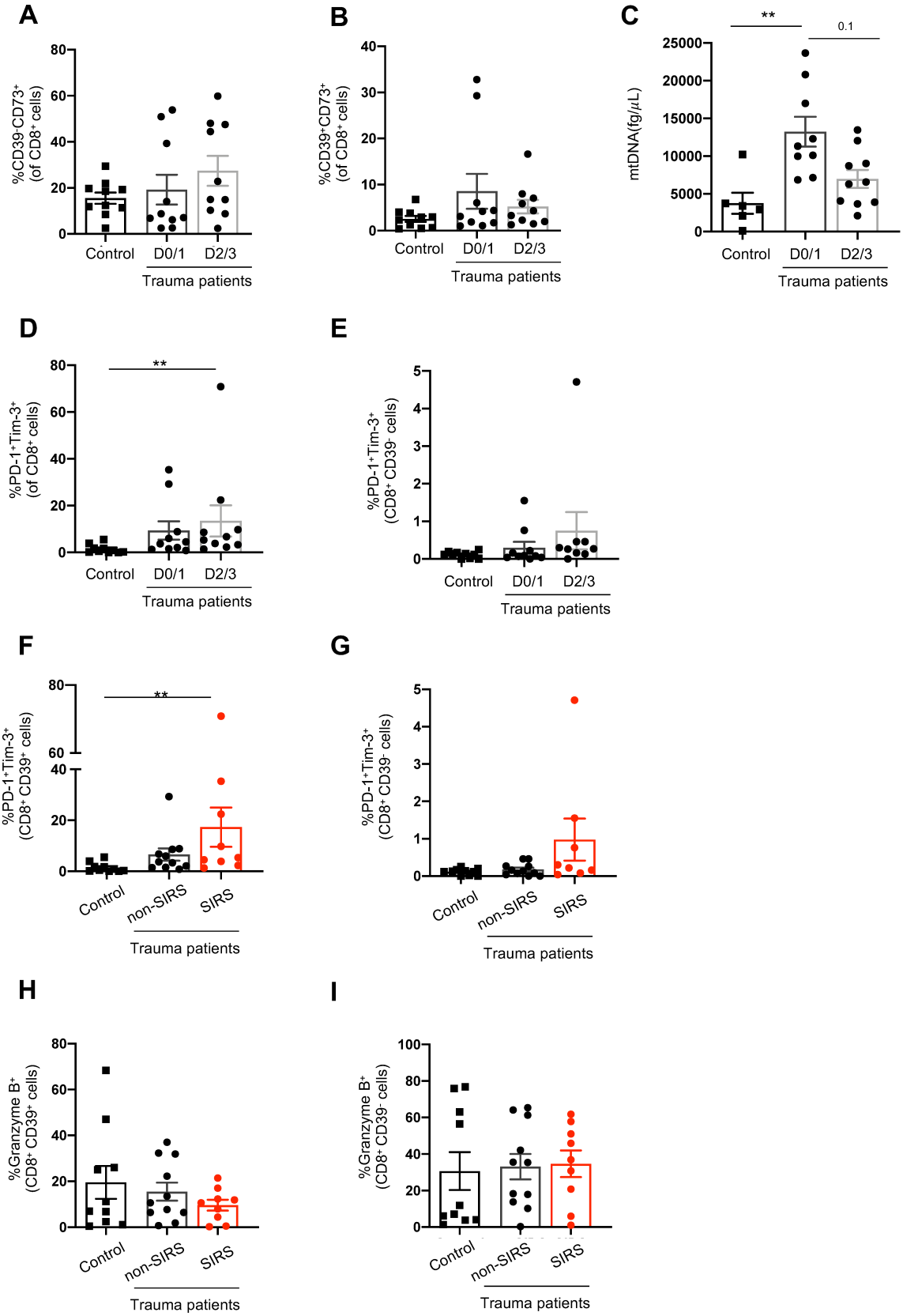
A
%CD39-CD73+ (of CD8+ cells)
Control
D0/1
D2/3
Trauma patients
B
%CD39+CD73+ (of CD8+ cells)
Control
D0/1
D2/3
Trauma patients
C
**
0.1
mtDNA(fg/μL)
Control
D0/1
D2/3
Trauma patients
D
**
%PD-1+Tim-3+ (of CD8+ cells)
Control
D0/1
D2/3
Trauma patients
E
%PD-1+Tim-3+ (CD8+ CD39- cells)
Control
D0/1
D2/3
Trauma patients
F
**
%PD-1+Tim-3+ (CD8+ CD39+ cells)
Control
non-SIRS
SIRS
Trauma patients
G
%PD-1+Tim-3+ (CD8+ CD39- cells)
Control
non-SIRS
SIRS
Trauma patients
H
%Granzyme B+ (CD8+ CD39+ cells)
Control
non-SIRS
SIRS
Trauma patients
I
%Granzyme B+ (CD8+ CD39- cells)
Control
non-SIRS
SIRS
Trauma patients

Supplementary Table 1. Demographic and clinical data of trauma patients.

Gender	Mechanism of injury	Injured body system	ISS Score	Hospitalization (days)	ICU length (days)	Requiring ICU treatment	Requiring mechanical ventilation
Male	Motor vehicle accident	Head/Brain, Lung/ Chest Wall	25	5	0.7	Yes	No
Male	Fall	Spine	6	3	1.4	Yes	Yes
Male	Fall	Abdominal	17	3	1.1	Yes	No
Male	Motor vehicle accident	Spine, Lung/ Chest Wall, Pelvis / Extremities Injury	17	5	0.7	Yes	Yes
Male	Motor vehicle accident	Lung/ Chest Wall, Pelvis / Extremities Injury	13	10	0	No	No
Male	Stab wound	Lung/ Chest Wall	10	5	0.38	Yes	No
Male	Gunshot wound	Pelvis / Extremities Injury	10	8	0	No	No
Male	Motor vehicle accident	Spine, Lung/ Chest Wall, Abdominal, Pelvis / Extremities Injury	24	23	13.8	Yes	Yes
Male	Motor vehicle accident	Head/Brain, Lung/ Chest Wall, Abdominal	22	7	1.79	Yes	Yes
Male	Fall	Head/Brain, Lung/ Chest Wall, Abdominal	21	10	3.39	Yes	Yes
Male	Motor vehicle accident	Head/Brain	75	3	1.69	Yes	Yes

Supplementary Table 2. Demographic and clinical data of control patients.

Gender	Hospitalization (days)	ICU length (days)	Requiring ICU treatment	Requiring mechanical ventilation
Male	4	0	No	Yes
Female	2	0	No	Yes
Female	6	1.3	Yes	Yes
Male	3	0	No	Yes
Female	8	0	No	Yes
Male	1	0	No	Yes
Male	8	0	No	Yes
Male	5	1.2	Yes	Yes
Male	2	0	No	Yes
Male	7	0	No	Yes

SUPPLEMENTARY MATERIALS

Supplementary Materials: Flow cytometry Antibodies.

Human studies: Anti-human CD8 APC/Cy7 (Clone SK1), anti-human CD39 FITC (Clone A1), anti-human CD73 APC (Clone AD2), anti-human CD279 (PD-1) Pacific Blue (Clone EH12.2H7), anti-human Tim-3 PE (Clone F38,2E2), anti-human CD152 (CTLA4) PE (Clone L3D10), anti-human CD45-RO PE/Cy7 (CloneUCHL1), anti-human Granzyme B APC (Clone QA16A02), anti-human IFNγ FITC (Clone 4S.B3), anti-human IL10 APC (Clone JES3-19F1), anti-human CD39-PE/Cy7 (Clone A1), anti-human CD73-PE (Clone AD2). All antibodies were from Biolegend, San Diego, CA); mouse studies: anti-mouse CD8a-APC/Cy7 (Clone: 53-6.7, Biolegend, San Diego, CA), anti-mouse CD39 PE/Cy7 (Cl9one 24DMS1, eBioscience, San Diego, CA), anti-mouse CD73-Pacific Blue (Clone TY/11.8, eBioscience, San Diego, CA), anti-mouse PD-1 PE (Clone 243, eBioscience, San Diego, CA), anti-mouse Tim-3 APC (Clone RMT3-23, Biolegend, San Diego, CA), anti-mouse CD152-BV605 (Clone UC10-4B9, Biolegend, San Diego, CA), anti-mouse CD44 APC (Clone IM7, eBioscience, San Diego, CA), anti-mouse IFNγ PE (Clone XM G1.2, eBioscience, San Diego, CA), anti-mouse IL10 APC (Clone JES5-16E3, Biolegend, San Diego, CA), anti-human/mouse Granzyme B PerCP-Cy5.5 (Clone QA16A02, Biolegend, San Diego, CA). LIVE/DEAD™ Fixable Violet Dead Cell Stain Kit for 405 nm excitation (Invitrogen™, Thermo Fisher Scientific).

Supplementary Figure 1: Representative flow cytometry gating strategy for blood-derived leukocytes in mice

(A) Lymphocytes are set in forward angle (FSC) versus right angle scatter (SSC). For selecting $CD39^+$ and $CD39^-$ cells histogram dot plots are used after gating for $CD8^+$ cells. (B) Representative dot plots for $CD39^-CD73^+$, $CD39^+CD73^+$ and $CD39^+CD73^-$ cells are shown for control (untreated) and MT treated mouse. Additionally, unstained controls are displayed for CD39 and CD73 staining. (C) Representative dot plots for Tim-3^+, PD-1^+Tim-3^+ and PD-1^+ cells are shown for control and MT treated mouse**.** Additionally, unstained controls are displayed for PD-1 and Tim-3 staining (D-E) To analyze the frequency of Granzyme B^+ cells and IL-10^+ cells, CD8 expressing cells were set in a Granzyme B or IL-10 versus CD8 staining.

Supplementary Figure 2: Representative flow cytometry gating strategy for lung-derived leukocytes in mice

(A) Lymphocyte populations are selected in forward angle (FSC) versus right angle scatter (SSC). For identifying $CD39^+$ and $CD39^-$ cells histogram dot plots are used after gating for $CD8^+$ cells. (B) Representative dot plots for $CD39^-CD73^+$, $CD39^+CD73^+$ and $CD39^+CD73^-$ cells and (C) for Tim-3^+, PD-1^+Tim-3^+ and PD-1^+ cells are shown for control (untreated) and MT treated mice. (D-E) The frequencies of Granzyme B^+ $CD8^+$ cells and IL-10^+ $CD8^+$ cells are displayed for control and MT treated mouse.

Supplementary Figure 3: Effect of intact whole mitochondria on $CD8^+$ T cells *in vitro.*

(A) ROS production and ATP release from extracellular mitochondria isolated from mouse hepatocytes are visualized using fluorescent dye MitoSOX™ and ATP probe 2-2 Zn (×100 objective; scale bar, 10 μm) before and after addition of succinate (20 mM). (B-C) The phenotype of $CD8^+$ T cells was assessed before and after addition of CD3/CD28 Dynabeads, in the absence (Control) or presence of adenosine (ADO) (50 μM), ATP (1mM) and mitochondria (MT) (50 μg/ml) for 24 hours. (B) Percentages of Granzyme B^+ cells within $CD8^+CD39^+$ cells are shown. Mean± SEM frequency of IFNγ (C), Tim-3^+ (D) and PD-1^+ (E) within $CD8^+$ cells are displayed. (F) Frequency of CTLA-4^+ cells within blood derived $CD8^+$ T cells in control (untreated) and MT treated mice is represented. P value calculated by Kruskal–Wallis tests followed by Dunn's multiple comparisons. * $p < 0.05$.

Supplementary Figure 4: Mitochondria and bacteria cause lung injury with loss of $CD8^+$ T cells and accumulation of pro-inflammatory immune cells.

(A) Alveolar cells were obtained from mitochondria (MT, n=7), mitochondria and bacteria (MT+BAC, n=8) and bacteria (BAC, n=8) treated mice and stained for flow cytometry analysis. Mean± SEM frequency of $CD11b^+$, $Ly6G^+$, $CD4^+$ and $CD8^+$ cells within lung derived $CD45^+$ cells are shown. (B-C) Representative images of immunohistochemical

staining of Ly6G neutrophils (B) and CD8 cells (C) in lung sections obtained from untreated (control) and MT, BAC and MT+BAC treated wild type mice (×20, scale bar: 100 µm). P value obtained using Kruskal–Wallis tests followed by Dunn's multiple comparisons. ** $p < 0.01$.

Supplementary Figure 5: Mitochondria and bacteria induce Granzyme B^+ and decrease IL-10^+ production in lung derived $CD39^+$ $CD8^+$ T cell subsets.

Mice were untreated (controls, n=4), or treated with MT (n=7), MT+ BAC (n=8) and BAC (n=8). Lung derived $CD8^+$ T cells obtained from these mice, were subdivided into $CD39^+$ and $CD39^-$ subpopulations. (A, B) Frequencies of Granzyme B^+ cells are represented within lung derived $CD39^+CD8^+$ and $CD39^-CD8^+$ lymphocytes. (C, D) Percentage of $IL10^+$ producing cells within $CD39^+CD8^+$ and $CD39^-CD8^+$ cells are shown. (E, F) Frequency of $PD\text{-}1^+Tim\text{-}3^+$ cells among $CD39^+CD8^+$ and $CD39^-CD8^+$ cells. Data represent mean± SEM. P value obtained using Kruskal–Wallis tests followed by Dunn's multiple comparisons. * $p < 0.05$; ** $p < 0.01$.

Supplementary Figure 6: Characterization of CD8 T cell phenotype in trauma patients.

Frequencies of $CD39^-CD73^+$ (A) and $CD39^+CD73^+$ (B) within circulating $CD8^+$ T cells in controls (n=10) and trauma patients (n=10 per group). (B) Circulating levels of mitochondrial DNA (fg/μL) in controls and trauma patients at day 0/1 and day 2/3. Frequencies of $PD\text{-}1^+Tim\text{-}3^+$ cells within $CD8^+$ cells (D) and $CD39^-CD8^+$ cells (E) in controls and trauma patients. Percentages of $PD\text{-}1^+Tim\text{-}3^+$ cells within $CD39^+CD8^+$ (F) and $CD39^-CD8^+$ lymphocytes (G) are shown. Frequencies of Granzyme B^+ cells within $CD39^+CD8^+$ (H) and $CD39^-CD8^+$ lymphocytes (I) are displayed. Data represent mean± SEM. P value obtained using Kruskal–Wallis tests followed by Dunn's multiple comparisons. ** $p < 0.01$.

Supplementary Video 1: MitoTracker™ staining following addition of CCCP, exogenous ATP and apyrase

Freshly isolated liver derived mitochondria were stained with MitoTracker™ and were imaged by video fluorescence microscopy. Uncoupling agent CCCP (10µM) was added after 10 sec. 100x oil objective, frame rate: 10 frame per 1 sec.

Supplementary Video 2: ATP Probe staining following addition of CCCP, exogenous ATP and apyrase

ATP release from freshly isolated liver derived mitochondria were imaged by using ATP probe 2-2 Zn and recorded by video microscopy following addition of 10µM CCCP (10 sec), exogenous 1mM ATP (50 sec) and 10 U/ml apyrase (70 sec). 100x oil objective, frame rate: 10 frame per 1 sec.

Supplementary Video 3: MitoSOX™ staining after addition of succinate

Liver derived mitochondria were visualized with MitoSOX™ and after addition of 20 mM succinate (11 sec). 100x oil objective, frame rate: 10 frame per 1 sec.

Supplementary Video 4: ATP Probe staining after addition of succinate

ATP release was monitored by video fluorescence microscopy following treatment with 20 mM succinate (12 sec). 100x oil objective, frame rate: 10 frame per 1 sec.